Lifetime statistics for single Kevlar 49 filaments in creep-rupture

H. DANIEL WAGNER*, PETER SCHWARTZ‡, S. LEIGH PHOENIX
Sibley School of Mechanical and Aerospace Engineering, and ‡Department of Textiles and Apparel, Cornell University, Ithaca, New York 14853, USA

Experimental data are presented for the lifetime of single Kevlar 49 filaments under moderate to high stress levels at standard ambient conditions (21° C, 65% r.h.). Filaments were drawn from two spools, A and B, taken from the same production lot. Previously we found that filaments from spool A were 7% lower in mean strength but much less variable in diameter than filaments from spool B; however, the respective variabilities in failure stress were equivalent. The lifetime data were interpreted in light of a previously developed kinetic model embodying Weibull failure statistics and power law dependence of lifetime on stress level. As predicted, lifetime data at each stress level generally followed a two-parameter Weibull distribution with a shape parameter value near 0.2. Based on absolute stress levels, the filaments drawn from spool B had a Weibull scale parameter for lifetime about ten times greater than those from spool A; however, when the stress-levels were normalized by the respective Weibull scale parameters for short-term strength, these differences disappeared. With respect to power law dependence of lifetime on stress level, three distinct time domains emerged, each marked by a different power law exponent. Similar behaviour was observed earlier for preproduction Kevlar 49/epoxy strands, and the values for the power law exponents for the filaments agree closely with those for the strands.

1. Introduction

Kevlar 49§ fibrous composites are routinely fabricated to have strengths above 1.5 GPa (200 × 10^3 psi), but in many high performance applications (cables, pressure vessels, flywheels) one would like to sustain such stresses for long time periods. Thus the internal creep-rupture processes are of interest.

In the early 1970s when Kevlar fibre was first introduced by du Pont, little was known about its molecular structure and morphology and kinetic models for creep-rupture were of questionable applicability. At the same time, models combining filament lifetime statistics and matrix viscoelasticity to predict composite lifetime were almost nonexistent. Thus Lawrence Livermore National Laboratory embarked on long-term creep-rupture experiments on Kevlar 49/epoxy strands since these were the building blocks of the final composite structures, yet were small enough to test in large numbers.

Phoenix and Wu [1] give one interpretation of the strand results, and show complex behaviour for the lifetime distributions and their dependence on stress level. For example, strength and lifetime results are affected by the type and volume fraction of the matrix in a way not predicted by the rule of mixtures. Using a power law relationship to relate median lifetime to stress level they show a factor of two reduction in the value of the exponent in going from the short-time regime (before 100 h) to the long-time regime, and the

coefficient of variation of lifetime also decreases by a factor of two. Similar results are also seen for Kevlar 49/epoxy pressure vessels. Clearly the epoxy matrix plays an important role in both strength and creep-rupture, but this cannot be determined without first having data on the individual Kevlar 49 filaments. Phoenix and Wu [1] did perform limited indirect experiments on filaments but with inconclusive results.

Recently, Phoenix and co-workers [2–5] have developed micromechanical models for composite strength and lifetime. Extensions of these models show promise of predicting composite lifetime distributions from fibre strength and lifetime statistics, matrix viscoelastic behaviour and interphase failure kinetics. At the same time, considerable recent work has been done towards understanding the supra-molecular structure, degree of crystallinity and larger scale morphology of Kevlar 49 filaments [6–9], and attempts have been made to use this knowledge to explain their creep and fracture topography [10, 11].

Historically, various kinetic models have been proposed to explain creep-rupture in polymeric materials. One approach has been to consider intermolecular chain slippage as the underlying mechanism [12–14]. These models built on rate process formulations as given by Eyring [15] and Tobolsky and Eyring [16].

A second approach has been to consider

---

macromolecular chain scission as the underlying failure mechanism. This idea seems to have originated with Tobolsky and Eyring [16] and was further developed by Coleman [17]. Similar kinetic models have been proposed [18, 19] and have been extended to include local stress transfer in a polymer network [20, 21].

The above models for chain slippage are similar in parametric form to those for chain scission and, as pointed out by Henderson et al. [22], it is difficult to distinguish among them solely on the basis of lifetime data. However, sometimes the observed activation energies are low enough to rule out chain scission as the dominant process. In this regard Smook et al. [23] argued convincingly for chain slippage as the dominant process in ultra-high strength polyethylene fibres. Indeed, it is reasonable to expect that both kinetic processes occur simultaneously, and interact to yield the final fracture event, thus confounding the interpretation of lifetime data (see [24–26]).

A somewhat different approach to creep-rupture lifetime of polymers has been developed by Christensen and co-workers [27–30], on a viscoelastic kinetic formulation of the classical crack stability problem of fracture mechanics. Recently it was applied to Kevlar 49/epoxy composites [28, 30].

As alluded to earlier, an important aspect of creep-rupture in Kevlar 49 composites (and other polymers) is the large inherent variability in the lifetime data. Phoenix and Wu [1] show that a Weibull distribution fits lifetime data rather well with large coefficients of variation ranging from 50% to 150%. But for single Kevlar 49 filaments, the variability appears to be about four times larger. In fact, roughly the same ratio also holds for short-term strength. Most of the models described earlier do not deal with this variability, but the model we describe later will do so comprehensively.

With the above as motivation, we have embarked on an experimental programme to determine the statistics for creep-rupture lifetime of single Kevlar 49 filaments. Here we report some results obtained at room temperature. Apart from long-term failure, we would like to understand the relationship between the distributions for short-term strength and long-term life.

Regarding short-term strength, an extensive study of statistical variability in the strength of single Kevlar 49 filaments was recently performed in our laboratory [31]. We found that their failure stresses can be adequately fitted to a two-parameter Weibull distribution. However, we also found significant variability in the linear density (and diameter) of filaments taken from a cross-section of yarn. Also, both the extent of this variability, and the mean filament strength differed from spool-to-spool. In view of these differences, and the theoretical link between the distributions for short-term strength and long-term life, we conjectured that spool-to-spool differences would also be revealed in filament lifetime behaviour. In fact, significant spool-to-spool variation in the lifetime of Kevlar 49/epoxy pressure vessels was noticed by Gerstle and Kunz in a recent study [32], and in one case anomalous results were connected to the atypical size distribution of the filaments.

2. Statistical model for filament failure

In this section we describe our theoretical model for filament strength and lifetime. The parametric form of the model was originally proposed by Coleman [33], and theoretical arguments supporting this form were given by Phoenix and co-workers [3–5]. Here we review a few key features.

2.1. Theoretical background

From the theory of absolute reaction rates the mean time, τ, between failure events (slippage or scission) for a given molecule under constant stress $\sigma \geqslant 0$ follows

$$\tau(\sigma) = \tau_0 \exp\left[U(\sigma)/(k\tilde{T})\right] \tag{1}$$

where τ_0 is a period of bond vibration, k is Boltzmann's constant, $\tilde{T}$ is absolute temperature and $U(\sigma)$ is the thermal activation energy required for the event as a function of stress σ. (In the model of Tobolsky and Eyring [16] $1/\tau_0$ is the frequency factor $k\tilde{T}/h$, where h is Planck's constant.) In fact the time until such an event occurs is random and follows an exponential distribution with hazard rate $1/\tau(\sigma)$.

For $U(\sigma)$, the almost universally accepted form is the linear approximation

$$U(\sigma) \simeq U_0 - \lambda\sigma \tag{2}$$

where U_0 is the activation energy in the absence of stress and λ is the so-called activation volume. This approximation seems to have originatred with Eyring [15], and is the basis for all the previously discussed lifetime models [12–26].

Despite the widespread acceptance of the linear approximation in Equation 2 it has been pointed out by several authors that the function $U(\sigma)$ actually has significant curvature, especially in the case of chain scission, and this curvature has led to anomalies in the interpretation of creep data (see the Appendix in [4] for extensive discussion on this). Furthermore, the mathematical simplicity expected to result from the linear form (Equation 2) fails to materialize when one considers local molecular stress redistribution and time varying stress histories [3, 4, 34]. That being the case, Phoenix and Tierney [4] have argued for the approximation

$$U(\sigma) \simeq -\tilde{U}_0 \log\left(\sigma/\tilde{\sigma}_0\right) \tag{3}$$

where $\tilde{U}_0$ and $\tilde{\sigma}_0$ are positive constants, and they showed a good fit in the case of the Morse potential function. This logarithmic approximation has several advantages: first, for a polymer under constant stress, the commonly used power law relationship emerges for the dependence of lifetime on stress level; that is, a linear relationship (with negative slope) emerges between stress and life using log–log coordinates. Second, when failure is preceded by multiple events involving local stress redistribution among molecules, the above power law relationship remains intact. Third, more sophisticated statistical formulations which can account for variability in lifetime are amenable to time-varying loads. (See Coleman [35] for illustration of these last two points.) Thus the logarithmic approximation in Equation 3 does not

suffer from difficulties arising from the use of the linear approximation in Equation 2, and is the basis for our model for fibre failure.

2.2. Details of the model

The distribution function for the failure time of a single filament, loaded according to the stress history $l(t)$, $t \geqslant 0$, is assumed to be of the form

$$F(t; l) = 1 - \exp\left(-\Psi\left\{\int_0^t \kappa[l(u)] \, du\right\}\right), \quad t \geqslant 0 \tag{4}$$

where $\Psi(\cdot)$ and $\kappa(\cdot)$ are special functions defined as follows: following Coleman [33] we call $\kappa(x)$, $x \geqslant 0$ the breakdown rule and we work exclusively with the power law breakdown rule

$$\kappa(x) = \gamma x^{\varrho}, \quad x \geqslant 0 \tag{5}$$

where ϱ and γ are positive constants. Also, we call $\Psi(x)$, $x \geqslant 0$ the shape function, and to impart the commonly observed Weibull features to lifetime and strength, we assume the Weibull shape function

$$\Psi(x) = \mu x^s, \quad x \geqslant 0 \tag{6}$$

where μ and s are positive constants.

As mentioned earlier, the above model was proposed by Coleman [33] on phenomenological grounds, but Phoenix and co-authors [3–5] were able to justify the basic form. In particular Phoenix [3] has considered a crystal model for the failure of a single filament wherein the molecules are aligned in parallel and fail at random points due to chain scission. Local elastic stress redistribution occurs at these molecular breaks leading in time to growing clusters of breaks, one of which grows catastrophically to fail the filament. The general form of Equation 4 results with aspects as follows: the power law breakdown rule, Equation 5, is essentially a molecular failure rate, and arises upon combining Equations 1 and 3 whereby

$$\gamma = \tau_0^{-1} \tilde{\sigma}_0^{-\tilde{U}_0/(k\tilde{T})} \tag{7}$$

and

$$\varrho = \tilde{U}_0/(k\tilde{T}). \tag{8}$$

The integral form in Equation 4 to handle time varying stresses arises from a special factorization property of the power law breakdown rule which is useful in molecular stress redistribution settings. The approximate Weibull shape of $\Psi(\cdot)$ arises from the crystal model, and Phoenix and Kuo [5] showed how finite but random molecular length leads to values of the Weibull exponent s which are less than unity, as observed experimentally. Lastly, the constant μ is proportional to filament volume (and thus its length) but it also involves the molecular stress redistribution constants and ϱ. In any case the above model, generated from the chain scission point of view, has the parameters and form needed to interpret our data.

Combining Equations 4, 5 and 6, the filament model reduces to

$$F(t; l) = 1 - \exp\left\{-\mu\gamma^s\left[\int_0^t l(u)^{\varrho} \, du\right]^s\right\}, \quad t \geqslant 0 \tag{9}$$

For creep-rupture lifetime we consider the constant stress history $l_1(t) = \mathscr{L}$ for $t \geqslant 0$ and stress level $\mathscr{L}$. The lifetime distribution $F(t; l_1)$ reduces to the Weibull distribution

$$F(t) = 1 - \exp[-(t/r)^s], \quad t \geqslant 0 \tag{10}$$

with shape parameter s and scale parameter

$$r = \mathscr{L}^{-\varrho}\mu^{-1/s}\gamma^{-1}. \tag{11}$$

Notice that a plot of log (r) against log $(\mathscr{L})$ yields a straight line with negative slope $-\varrho$.

For short-term strength we consider the linearly increasing stress history $l_2(t) = \mathscr{R}t$, $t \geqslant 0$ where $\mathscr{R}$ is the loading rate. Letting T be the failure time, we may use Equation 9 to calculate $F(t; l_2)$. However, we want the distribution function $F^*(x)$, $x \geqslant 0$ for the failure stress $X = \mathscr{R}T$, and this is clearly $F^*(x) = F(x/\mathscr{R}; l_2)$. The final result is that the filament strength follows the Weibull distribution

$$F^*(x) = 1 - \exp[-(x/a)^b], \quad x \geqslant 0 \tag{12}$$

with shape parameter $b = s(\varrho + 1)$, and scale parameter

$$a = [\mathscr{R}(\varrho + 1)/(\gamma\mu^{1/s})]^{1/(\varrho+1)} \tag{13}$$

Suppose that the Weibull scale parameter for strength a is known at stress rate $\mathscr{R}$ and we want the Weibull scale parameter r for lifetime at the stress level $\mathscr{L} = a$. This is easily determined from Equations 11 and 13 to be

$$r = a/[\mathscr{R}(\varrho + 1)] \tag{14}$$

Thus, r is the time taken in the tension test to reach the stress a divided by $\varrho + 1$.

We note that the model of Christensen and co-workers [29] has a similar power law framework and likewise generates Weibull distributions for both strength and lifetime, but with $b = s\varrho$. This is not an important difference since $\varrho \gg 1$ is typical. However, their Weibull nature arises by assuming it to be true for short-term strength whereas ours is an approximation obtained from more fundamental analysis [3–5]. At the same time, their ϱ has a different kinetic origin; it is twice the reciprocal of the exponent in the power law creep function assumed for the material.

Lastly, we consider the question of residual strength for survivors of a creep-rupture experiment. Suppose we apply the load history

$$l_3(t) = \begin{cases} \mathscr{L} & \text{for } 0 \leqslant t < t_c \\ \mathscr{R}(t - t_c) & \text{for } t \geqslant t_c \end{cases} \tag{15}$$

to a set of filaments; this amounts to running the creep-rupture experiment up to time t_c and performing a strength test after time t_c on the survivors. Letting

$$\mathscr{A} = \mathscr{L}^{\varrho} t_c \tag{16}$$

and

$$\mathscr{B} = \int_{t_c}^t [\mathscr{R}(u - t_c)]^{\varrho} \, du$$

$$= \mathscr{R}^{\varrho}(t - t_c)^{\varrho+1}/(\varrho + 1), \tag{17}$$

we may use Equations 9 and 15 to show that the

probability an arbitrary filament survives to time t_c is exp $\{-\mu\gamma^s\mathscr{A}^s\}$ whereas the probability it survives past time $t > t_c$ is exp $\{-\mu\gamma^s(\mathscr{A} + \mathscr{B})^s\}$. The probability of survival past time $t > t_c$ given survival to t_c is the ratio of the latter probability to the former, namely exp $\{-\mu\gamma^s(\mathscr{A} + \mathscr{B})^s + \mu\gamma^s\mathscr{A}^s\}$. Letting $T > t_c$ be the failure time, the associated failure stress is $X = \mathscr{R}(T - t_c)$. Thus by putting $x = \mathscr{R}(t - t_c)$ for $\mathscr{B}$ in the above ratio, and noting that the probability of failure is one minus the probability of survival, we obtain the distribution function for the strength of survivors to time t_c which is

$$F_c^*(x) = 1 - \exp\left(-\mu\gamma^s\{\mathscr{L}^\varrho t_c\right.$$
$$+ x^{\varrho+1}/[\mathscr{R}(\varrho + 1)]\}^s + \mu\gamma^s(\mathscr{L}^\varrho t_c)^s),$$
$$x \geqslant 0 \tag{18}$$

This distribution, which we call the residual strength distribution, is not a Weibull distribution, but reduces to Equation 12 for $t_c = 0$.

Consider now the median residual strength x_c^* which we obtain by solving $F_c^*(x_c^*) = 1/2$. The result is

$$x_c^* = [\mathscr{R}(\varrho + 1)/\gamma]^{1/(\varrho+1)}\{[(\gamma\mathscr{L}^\varrho t_c)^s + \mu^{-1} \log 2]^{1/s}$$
$$- \gamma\mathscr{L}^\varrho t_c\}^{1/(\varrho+1)} \tag{19}$$

Now the median strength x^* for the virgin fibres is simply Equation 19 with $t_c \equiv 0$, i.e.

$$x^* = [\mathscr{R}(\varrho + 1)/\gamma]^{1/(\varrho+1)}(\mu^{-1} \log 2)^{1/[s(\varrho+1)]} \tag{20}$$

Our interest is in the fractional change in residual strength which we define as $\Delta = (x_c^* - x^*)/x^*$. Using Equations 11, 13, 19, and 20 we arrive at

$$\Delta = \frac{\{[(t_c/r)^s + \log 2]^{1/s} - (t_c/r)\}^{s/b}}{(\log 2)^{1/b}} - 1 \tag{21}$$

It can be shown that Δ is positive for $s < 1$ and negative for $s > 1$ where we recall s is the Weibull shape parameter for lifetime.

3. Experimental procedure

In the present study we wanted to be able to apply a constant stress to a large number of single filaments simultaneously so we could generate a significant amount of data in a reasonable time period. For this purpose, we build a creep-rupture setup with stations for 48 filaments, with the individual loads applied by hanging weights. These weights were individually tailored at a given stress level because of linear density variations from filament to filament as noted in [31]. The filaments were actually suspended from microswitches which upon failure triggered a microcomputer timing system with printer.

In a previous study [31], we accumulated a substantial amount of information on distributions for the strength and linear density of Kevlar 49 single filaments. In particular, two spools from a common lot (no. 74048), herein labelled A and B for consistency with our previous study, possessed significant differences in behaviour. When compared to those from spool B, filaments from spool A had 7% lower mean strength but one-third the coefficient of variation in

their linear densities. These two spools were used in the present study.

To prepare specimens for each stress level we first removed 48 filaments from segments of yarn from each spool, using a procedure outlined in [31]. Upon extraction, each filament was mounted on light cardboard tabs (ASTM D3379) using common epoxy cement (3M). The gauge length used was 5 cm. The linear density (mass/unit length) of an adjacent portion of each filament was measured using the vibroscope method (ASTM D1577-79), thus giving us a precise though indirect measurement of the filament cross-sectional area (assuming a specific gravity of 1.44 for Kevlar 49).

Each set of 48 filaments was assigned a stress level set to be a given fraction of the Weibull scale parameter for strength for the corresponding spool as determined in [31]. (The respective scale parameter values were 3270 MPa for spool A and 3530 MPa for spool B.) In what follows these fractions are called stress ratios. For spool A we ran four lifetime sets at the respective stress ratios 0.79, 0.84, 0.89 and 0.94 whereas for spool B we ran sets at the ratios 0.74, 0.79, 0.84 and 0.89. Thus the ratios 0.79, 0.84 and 0.89 were set to be the same for both spools for purposes of comparing their lifetime statistics.

Using the linear density measurements, each filament was assigned a specially trimmed, hanging weight (bolt wrapped with lead solder) measured using a laboratory scale having an accuracy of 0.01 g. By comparison the weights for the lowest stress level were about 30 g.

As mentioned earlier, we performed the creep-rupture experiments on a specially designed apparatus built in our laboratory. Its main features are illustrated schematically in Fig. 1, where only one station is shown for clarity. The apparatus consists of a fixed frame and a moveable rack which can be positioned vertically at will. Single pole, double throw microswitches are fastened to the upper part of the frame; the top of the mounting tabs fitted easily into place with excellent alignment on the cantilever blade of the microswitches.

Just prior to the beginning of a test, the central portion of each tab was cut away, and, with the rack in the up position, the filament was carefully placed into position on the apparatus. The weights were set into holes machined in the rack so as to avoid any filament tension prior to the start of the experiment. To start the experiment we slowly lowered the rack using a simple mechanical system of cables and pulleys, taking care to minimize any impact loading. At the same time we activated a 4K RAM, Rockwell AIM-65 microcomputer which was connected to the microswitches. When a filament failed, the logic state of the corresponding microswitch was inverted; this event was detected by the computer and recorded by a printer (Fig. 2). This monitoring system allowed us to determine the identity of a filament and its lifetime, typically to within about 6 sec as discussed later. As expected, some filaments failed upon loading or within the first few seconds; these data were not discarded, but required special treatment in the data analysis as described later.

Figure 1 Schematic illustration of creep-rupture setup.
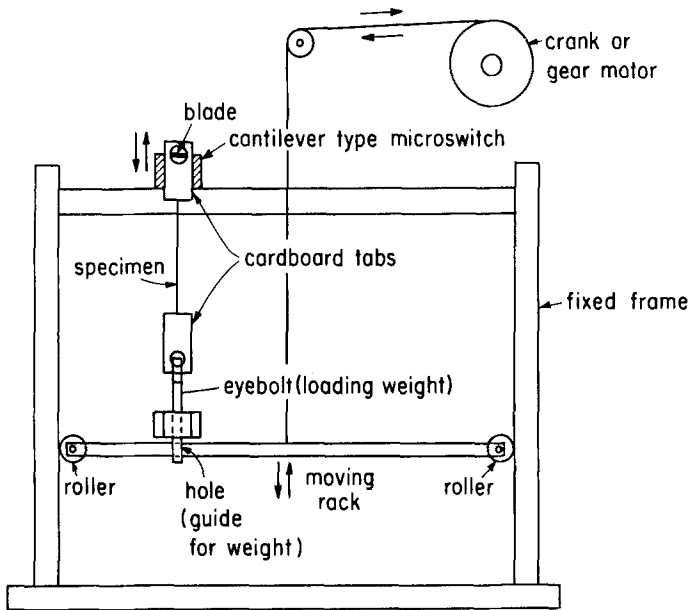
The creep-rupture experiments were run typically for about 192 h, at which time the tests were censored (Type I censoring), if indeed survivors remained. The tests were run at 21°C and 65% r.h. in a controlled room and, during the test, the apparatus was covered to avoid strength loss due to ultraviolet light, as had been previously seen [1].

Finally, in our previous study [31], filaments from spools A and B were found to follow a Weibull distribution for failure stress. For spool A the scale and shape parameters were respectively $a = 3270$ MPa and $b = 10.4$; for spool B the values were $a = 3530$ MPa and $b = 10.2$. These values are used later in the analysis of the results.

4. Results and discussion
First we consider statistics for the linear density (LD) of the filament samples in the various lifetime sets. Table I shows that the filaments from spool B have almost three times the variability of those from spool A, which is exactly what we found previously (Table 3 in [31]) for samples of similar size.

Next we consider the results of the lifetime tests. Table II contains information relevant to the testing. Shown for the various lifetime data sets are the stress ratios, the actual stress levels $\mathscr{L}$, the actual sample sizes n, the number of filaments which failed at the time of loading N_0, the number still surviving at the time of censoring N_c, the time of the last failure T_L, and the time of censoring t_c.

The lifetime results for the stress ratios 0.79, 0.84 and 0.89 for both spools are plotted, using Weibull coordinates, in Figs 3, 4 and 5 respectively. The graphs display only the lifetime data for which failure times are accurately known; that is, $N_0 + N_c$ points are missing on each (though all data are properly accounted for in the statistical analysis discussed shortly).

In Fig. 3 we have plotted an uncertainty band for the data from spool A arising from the following time resolution problems associated with the experimental apparatus: first, the accuracy of the computer printing device is about 1 sec. More important, the loading of samples is not instantaneous but takes about 3 sec in order to build up the stress. In addition, the starting of the computer was done manually and could have been in error by 2 or 3 sec. Thus specimen lifetimes are probably known only to within about 6 sec, and it would be unreasonable to attempt to plot lifetime values of this magnitude on the graphs.

A more subtle point is that the Weibull lifetime distribution (Equation 10), was derived assuming an idealized step loading at time zero, whereas the actual loading was a ramp loading followed perhaps by a slightly dynamic overload, all taking place over the first few seconds. In this latter situation Equation 9 would yield Equation 10 for times beyond these few startup seconds, except that $(t/r)^s$ would become $[(t + t_e)/r]^s$ for some constant t_e also of the order of a few seconds (provided the dynamic overload is small

TABLE I Linear density (LD) statistics for filament samples of various lifetime sets

Stress ratio	Spool A			Spool B		
	Mean LD $(\mathrm{mg\,m^{-1}})$*	c.v. (%)	n	Mean LD $(\mathrm{mg\,m^{-1}})$	c.v. (%)	n
0.74	—	—	—	0.182	27.4	46
0.79	0.170	11.5	48	0.185	27.9	46
0.84	0.168	10.6	48	0.175	23.4	48
0.89	0.172	11.7	48	0.189	32.8	48
0.94	0.175	10.5	48	—	—	—

*$1\,\mathrm{mg\,m^{-1}}$ is also 1 tex as in [31].

PRINTER

BATTERY BACKUP SYSTEM

AIM-65 MICROCOMPUTER

EVENT SCANNING MULTIPLEXER SYSTEM

CREEP RUPTURE SETUP

environmental chamber
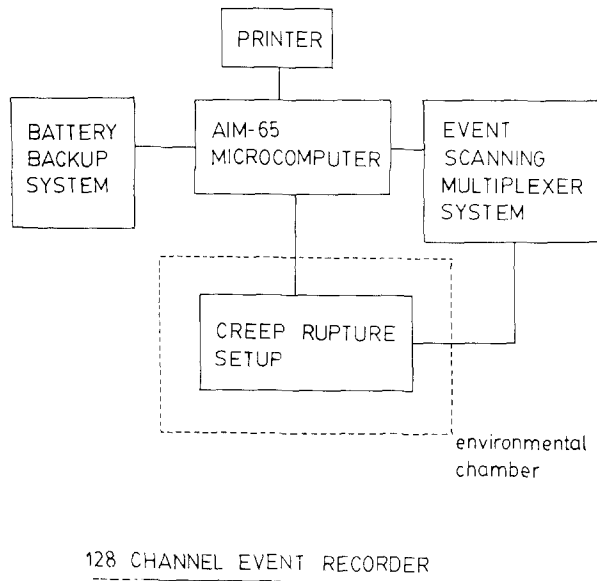
128 CHANNEL EVENT RECORDER

Figure 2 Block diagram of creep-rupture system.

and of short duration). Practically, the effect is to subtract t_e from all observed failure times. Thus the Weibull form in Equation 10, would be in error at times $t \sim t_e$; however, this error is unimportant if the scale parameter r is much larger than t_e, and s is not too small, since this error is confined to the extreme lower tail of $F(t)$. Later we see that r is typically many orders of magnitude greater than the range just suggested for t_e.

To estimate the Weibull scale and shape parameters (r and s) for lifetime at the various stress levels, we used a maximum likelihood estimation (MLE) procedure appropriate to censored samples. The resulting MLE values, $\hat{r}$ and $\hat{s}$, are given in Table III together with their respective 90% confidence intervals (CI) as computed using the methods of Nelson [36] and Meeker and Nelson [37]. Also given are the corresponding median lifetimes.

In the numerical analysis, a modified Newton–Raphson method was used to solve the MLE equations (see, for example, Nelson [36]). In applying the MLE procedure we arbitrarily assigned a lifetime value of 1 sec to all N_0 initial failures; in this regard we found the MLE procedure to be very robust in that varying these assigned times a few seconds had virtually no effect on the estimates, provided that the resulting estimate $\hat{r}$ was orders of magnitude larger, as was typically the case. In other words the MLE procedure weighs heavily the longer failure times nearer the sample median, and the time resolution difficulties discussed earlier are typically not a problem.

From the results presented, there appear to be significant differences between the results from spools A and B, as might have been anticipated from the strength results from our previous study [31]. The most obvious difference is that at any *absolute* stress level the lifetimes of filaments from spool B tend to be one to two orders of magnitude larger than those from spool A. This is also seen in Fig. 6, in which we plot the Weibull scale parameter estimate $\hat{r}$ against *absolute* filament stress level $\mathscr{L}$ using log–log coordinates. Also shown are the 90% CIs as given in Table III. On the other hand, Fig. 7 replots the Weibull scale parameter estimates $\hat{r}$ against stress ratio ϕ using log–log coordinates; and we see that these differences in lifetime virtually disappear. (In locating an equivalent $\hat{r}$ value for the strength scale parameter a, that is for $\phi = 1$, we were guided by Equation 14.) The remaining differences are in fact small compared with the sizes of the confidence intervals for these parameters as given in Table III, and shown in Fig. 6.

We attempted to apply a formal test of equality of the Weibull shape and scale parameters of these spools at each stress ratio, as proposed by Thoman and Bain [38]. Strictly speaking their test is valid only for uncensored data (there seems to be no corresponding test in the literature for censored samples), though our use of their test in this situation is conservative (in that a conclusion of equality of the parameters under their test implies the same under a more refined test but not vice versa). In applying the test separately at the stress ratio 0.79 and 0.89 we were able to rule out significant differences ($\alpha = 0.05$ level) in the respective Weibull shape and scale parameters for spools A and B; however, significant differences at the stress ratio 0.84 could not be ruled out, and may indeed emerge under a more refined test which takes censoring into account. Such results are not surprising in view of the amount of overlap in the respective confidence intervals (Table III). Later we suggest that the differences apparent at the stress ratio 0.84 are actually artifacts of initial dynamic overloads in the case of spool B.

On the other hand, two pieces of evidence suggest that the variability in lifetime for spool B is slightly larger than for spool A. First, looking at all the lifetime results together (Table III), the shape parameter estimates $\hat{s}$ at each stress level are consistently lower for spool B; in fact the average value of $\hat{s}$ for spool A is 0.222 (coefficient of variation = 7%) whereas the average value for spool B is 0.175 (c.v. = 17%). Second, in Table IV we show the observed number of instantaneous failures N_0 which occurred upon loading in the lifetime experiments; the

TABLE II Stress levels and other quantities associated with the lifetime data sets

Stress ratio	Spool A						Spool B					
	$\mathscr{L}$ (MPa)	n	N_0	N_c	T_L (h)	t_c (h)	$\mathscr{L}$ (MPa)	n	N_0	N_c	T_L (h)	t_c (h)
0.74	–	–	–	–	–	–	2626	46	7	21	671.8	691.9
0.79	2581	48	5	21	151.5	190.6	2791	46	6	20	178.8	178.8
0.84	2742	48	8	11	129.0	209.6	2955	48	20	11	122.6	191.9
0.89	2903	48	13	7	26.4	29.1	3119	48	16	3	95.9	192.0
0.94	3065	48	29	0	142.8	complete sample	–	–	–	–	–	–
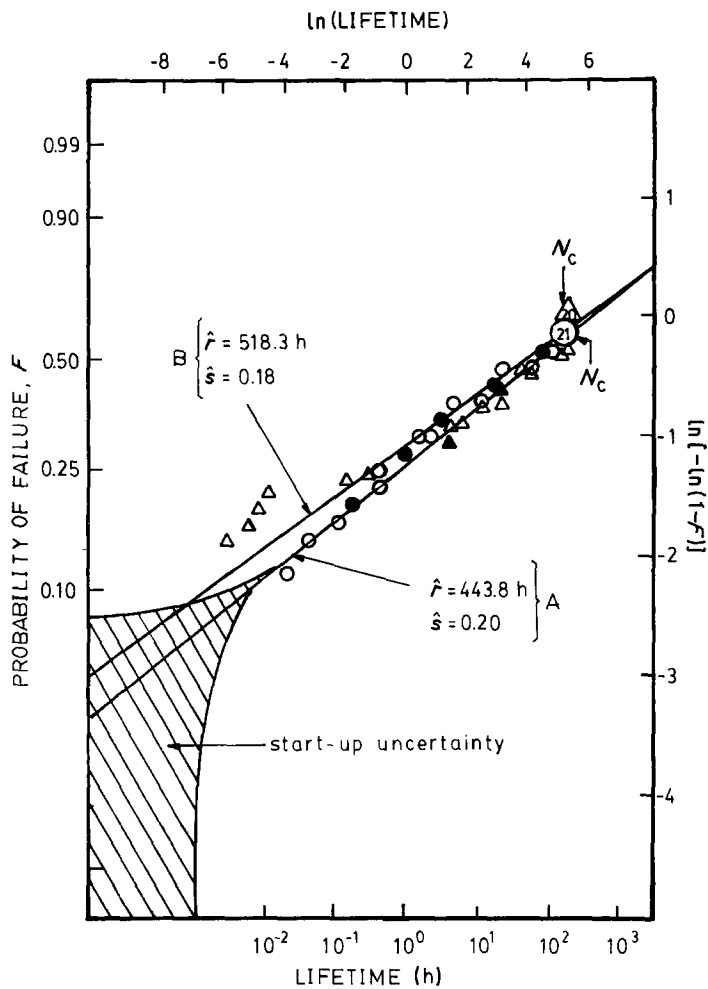
Figure 3 Weibull plot for 0.79 stress ratio. O, Spool A (N_0 = 5); △, Spool B (N_0 = 6); ●▲, multiple observations.
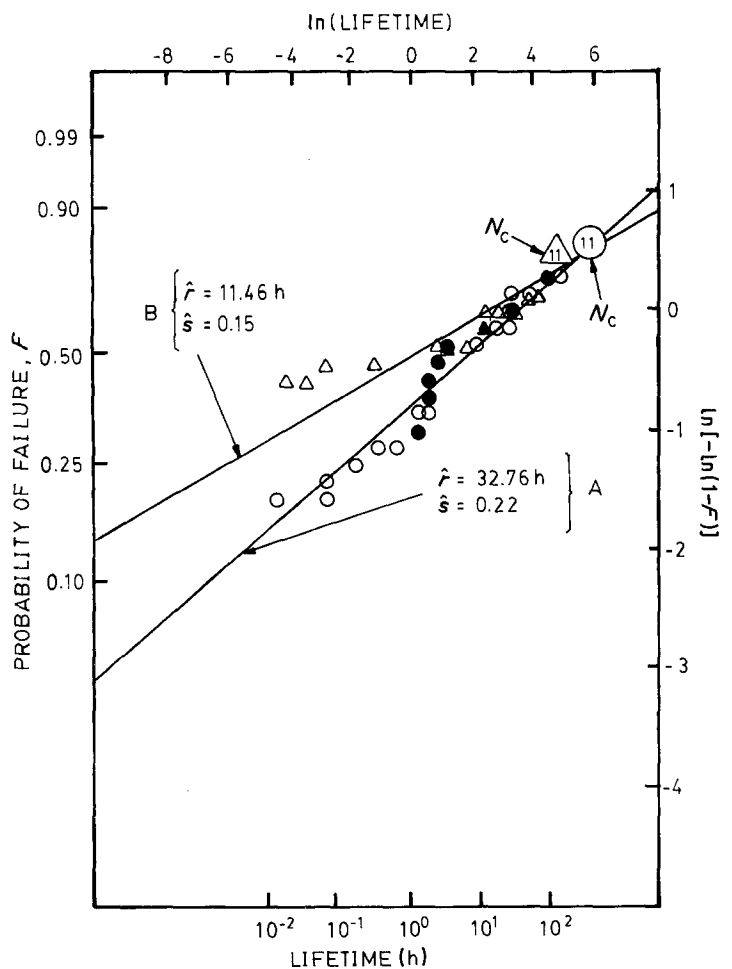
Figure 4 Weibull plot for 0.84 stress ratio. O, Spool A (N_0 = 8); △, Spool B (N_0 = 20); ●▲, multiple observations.

TABLE III MLE values and 90% confidence intervals (CI) for Weibull scale $\hat{r}$ and shape $\hat{s}$ parameters for filament lifetime

Stress ratio	Spool A			Spool B		
	$\hat{r}$ (h) (90% CI)	$\hat{s}$ (90% CI)	median (h)	$\hat{r}$ (h) (90% CI)	$\hat{s}$ (90% CI)	median (h)
0.74	—	—	—	2902 (310.1, 27 166)	0.157 (0.116, 0.212)	281.1
0.79	443.8 (85.11, 2314)	0.202 (0.152, 0.269)	72.18	518.3 (78.79, 3409)	0.183 (0.136, 0.246)	69.9
0.84	32.76 (9.74, 110.2)	0.221 (0.175, 0.279)	6.25	11.46 (1.828, 71.77)	0.146 (0.116, 0.185)	0.93
0.89	1.570 (0.55, 4.48)	0.245 (0.198, 0.303)	0.35	1.156 (0.3536, 3.777)	0.212 (0.174, 0.258)	0.21
0.94	0.0189 (0.006 10, 0.0586)	0.222 (0.185, 0.268)	0.0036	—	—	—

results for spool B tend to be larger at each stress level. In contrast, in our earlier study [31] we found no significant differences in the variability of the short-term strength (in units of stress) for the two spools.

Now the number of instantaneous failures N_0 at a given stress level follows a binomial distribution with mean $n_0 = np$ and standard deviation S.D. $= [np(1 - p)]^{1/2}$ where p is the probability of instantaneous failure of a given filament, and n is the number of filaments loaded. In Table IV we give the observed numbers N_0 together with the means n_0^* and respective standard deviations, S.D., calculated assuming p is determined by the Weibull distributions for strength obtained in [31]. (All numbers are rounded to the nearest integer.) We also give the means $n_0^{\ddagger}$ and respective standard deviations, S.D., calculated assuming p is determined by our fitted Weibull lifetime distributions

(Table III) evaluated at $t = 5$ sec (roughly the limit of resolution discussed earlier). In the case of spool A, the agreement is good except for the stress ratio 0.94 where the number observed seems high. However, in this case the fitted lifetime distribution does predict a number $n_0^{\ddagger}$ in accordance with n_0^* from the strength experiments. In the case of spool B, the agreement is quite reasonable except at the stress ratio 0.84 where the number of initial failures seems somewhat large, as indeed does $n_0^{\ddagger}$ relative to n_0^*.

These comparisons suggest perhaps that slight dynamic overloads occurred upon loading in some cases leading to appreciable values for the shift times t_e described earlier in this section. However, only in the case of spool B at the stress ratio 0.84 does it appear that the lifetimes were reduced sufficiently to moderately decrease the estimates for the Weibull
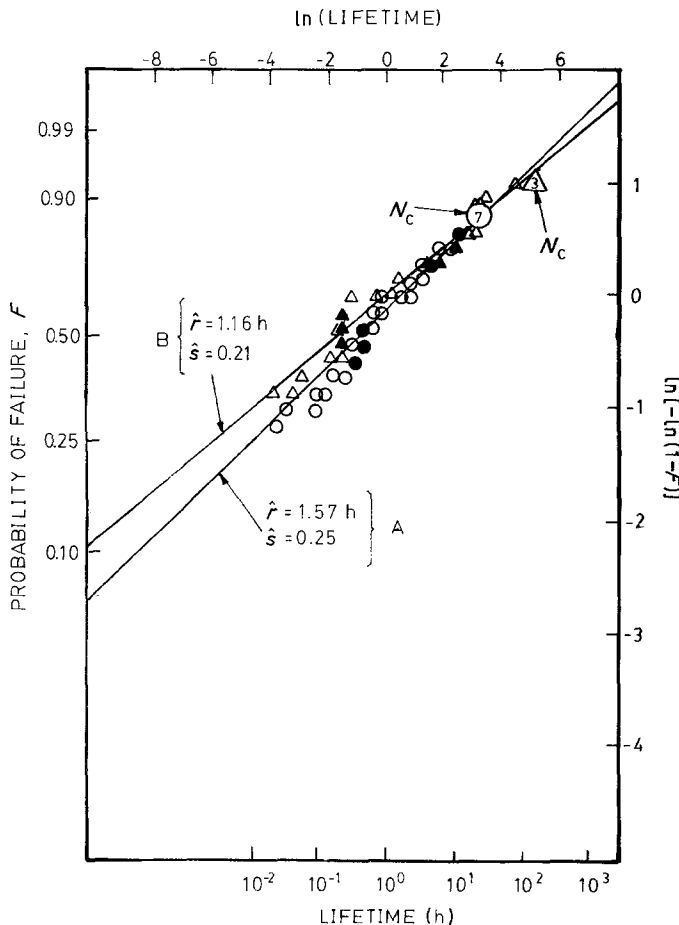

Figure 5 Weibull plot for 0.89 stress ratio. O, Spool A ($N_0 = 13$); △, Spool B ($N_0 = 16$); ●▲, multiple observations.

Stress ratio	Spool A			Spool B		
	N_0	$n_0^{*\dagger}$ (S.D.)	$n_0^{\ddagger\ddagger}$ (S.D.)	N_0	$n_0^{*\S}$ (S.D.)	$n_0^{\ddagger\ddagger}$ (S.D.)
0.74	—	—	—	7	3 (1)	4 (2)
0.79	5	4 (2)	4 (2)	6	4 (2)	4 (2)
0.84	8	8 (3)	5 (2)	20	8 (3)	11 (3)
0.89	13	12 (3)	8 (3)	16	12 (3)	10 (3)
0.94	29	20 (3)	21 (3)	—	—	—

†Based on Weibull strength distribution with a = 3270 MPa and b = 10.4 [31].
‡Based on Weibull lifetime distributions at t = 5 sec.
§Based on Weibull strength distribution with a = 3530 MPa and b = 10.2 [31].

shape and scale parameters. This last notion seems supported on Fig. 7 where the associated scale parameter $\hat{r}$ for ϕ = 0.84 appears to fall short of what one might anticipate. In fact, Fig. 4 shows that the actual lifetime observations for spool B which are of the order $\hat{r}$ = 11.46 h all tend to lie to the right of the Weibull plot for spool B, and indeed fall closer to that for spool A. Thus, for ϕ = 0.84, the true Weibull parameters r and s for spool B are possibly much closer to those for spool A than Figs. 4 (and 7) would indicate.

We tension tested the survivors of the lifetime experiments, that is, those specimens that had not failed at the time of censoring. According to Equation 21 their median strength x_c^* ought to be higher than the virgin medians x^*, since we observed $\hat{s}$ < 1. Table V compares our theoretical Δ and experimental $\hat{\Delta}$ values for the fractional increase in median strength of the survivors. To calculate these we used Weibull $\hat{r}$ and $\hat{s}$ values from Table III and Weibull $\hat{a}$ and $\hat{b}$ values from our earlier study [31]. Also, to get the $\hat{\Delta}$ values we divided the sample medians by x^* = $a(\log 2)^{1/b}$ and subtracted unity. In all cases the residual median strength exceeds the virgin median as predicted, and the numerical agreement is quite good in some cases.

Equation 11 of our theoretical model suggests that a plot of the lifetime scale parameter r against the stress level $\mathcal{L}$ plotted using log–log coordinates ought to be a straight line with slope $-\varrho$, where ϱ is the exponent in the power law breakdown rule of Equation 5. While Fig. 6 may tend to suggest such behaviour, Fig. 7 suggests a more complicated relationship. [Here $\log \phi$ = ($\log \mathcal{L}$ − constant) so that the slopes are unchanged in going from Fig. 5 to Fig. 6.] In Fig. 7 we have drawn three connecting lines to the data: one with ϱ = 85 for times up to 1 h, one with ϱ = 45 for times between 1 and 400 h, and one with ϱ = 30 for times after 400 h.

Phoenix and Wu [1] have observed very similar behaviour for Kevlar 49/epoxy strands and spherical pressure vessels (see Figs 4 and 10 in [1]; on their scales, the Weibull scale parameter for lifetime and the median lifetime will be virtually equivalent). In fact for the most complete data set, PRD49III strands (preproduction Kevlar 49) impregnated with a Union Carbide epoxy (ERL2258-ZZL0820), they show three connecting lines with the respective slopes ϱ = 85, ϱ = 45 and ϱ = 27, again with line transitions at about 1 and 400 h.

We mention that Christensen and Glaser [28] also analysed the data using their crack growth methodology, and arrived at ϱ = 45.6. However, the decrease
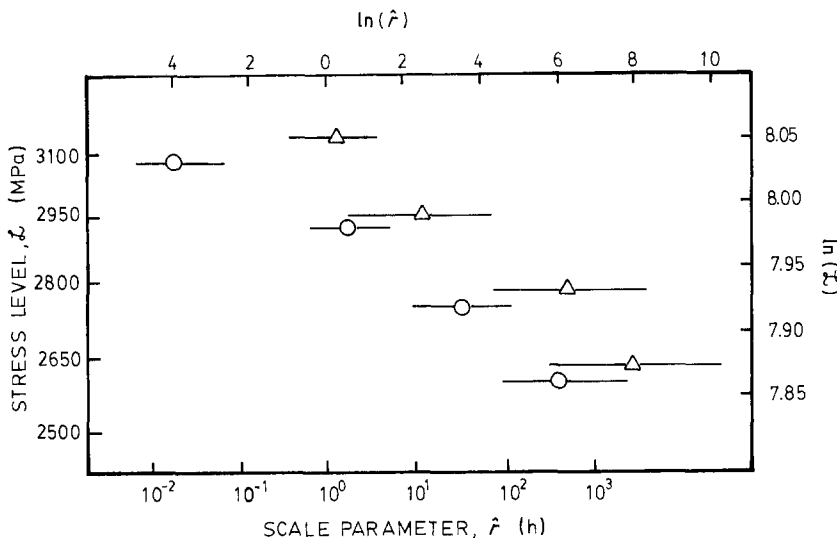

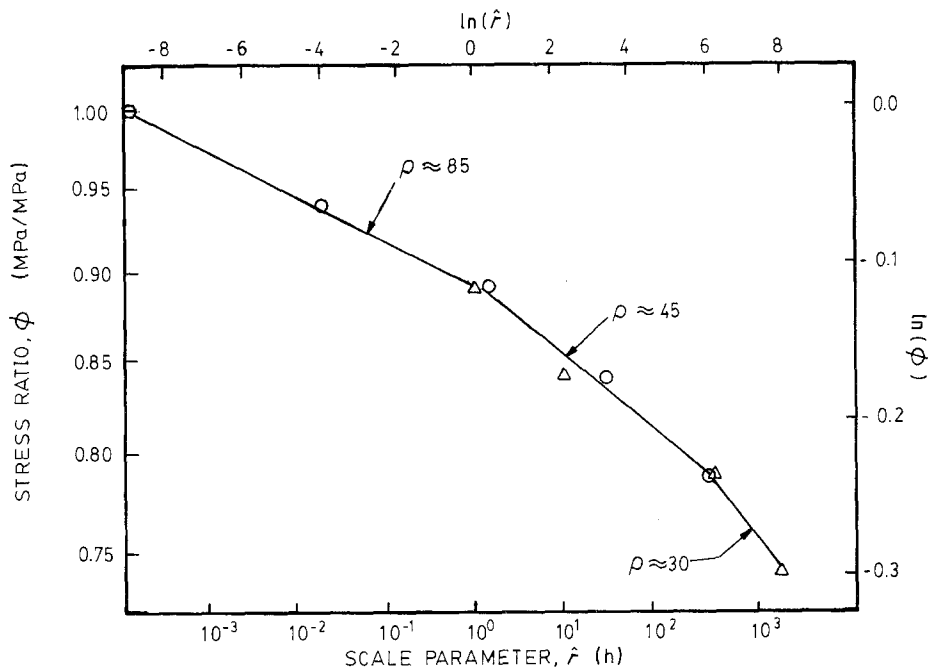Figure 6 Absolute filament stress plotted against Weibull lifetime scale parameter. O, Spool A, △, Spool B.

Figure 7 Filament stress ratio plotted against Weibull lifetime scale parameter. O, Spool A, △, Spool B; ⊙, tension tests.

in ϱ at later times was explained using a chemical degradation component of the model to account for the suspected effects of ultraviolet light. Our experiments were conducted in the dark.

In Equation 12, the Weibull shape parameter for strength is $b = s(\varrho + 1)$ so that the ratio of the Weibull shape parameters for strength $\hat{b}$ and lifetime $\hat{s}$ ought to be close in magnitude to the exponents ϱ on Fig. 7. Using the values for $\hat{s}$ in Table III and values for $\hat{b}$ given earlier we find $42 < \hat{b}/\hat{s} < 52$ for spool A and $48 \leqslant \hat{b}/\hat{s} \leqslant 70$ for spool B, which is of the right order of magnitude for ϱ; however, these ratios are erratic and furthermore do not predict the decrease in ϱ with decreasing stress level. The latter would require a steady increase in s with decreasing stress level (as was observed for Kevlar 49/epoxy strands by Phoenix and Wu [1]) and this does not happen. In fairness to the model, the time frame of the strength data determining $\hat{b}$ is orders of magnitude shorter than that for s at the lower stress levels, so that the molecular mechanism of failure could be different. Of course the erratic behaviour in $\hat{s}$ is not unexpected in view of the width of the confidence intervals in Table III. On the other hand, the values for both $\hat{b}$ and ϱ are roughly the same for spools A and B, yet the values for $\hat{s}$ are, on the whole, about 20% less for spool B. The model sheds no light on this difference.

In short-term strength, the Weibull shape par-

TABLE V Comparison of theoretical and experimental fractional increases in median strength of survivors of lifetime experiments

Stress ratio	Spool A		Spool B	
	Δ*	Δ̂	Δ*	Δ̂
0.74	—	—	0.079	0.044
0.79	0.080	0.058	0.081	0.059
0.84	0.12	0.140	0.12	0.048
0.89	0.14	0.230	—	—
0.94	—	—	—	—

*Calculated from Equation 21.

ameter for Kevlar 49/epoxy strands [1] is about three times that for single filaments (30 compared to 10). However, in lifetime, the corresponding ratio of the Weibull shape parameters seems to range from about three at high stress levels (0.6 compared to 0.2) to almost 10 at lower stress levels (2 compared to 0.2), again reflecting the constancy of s with stress level. Now in the micromechanical models of Phoenix and co-workers [3, 4] this composite to fibre ratio is determined by an equation (see Equation 6.23 in [4]) which involves the product $s\varrho$ in our notation, and approximately this ratio is inversely proportioned to $s\varrho$. If s is to remain constant as observed, the model would require that ϱ decrease by a factor of three as the stress level is decreased, and this is indeed what happens experimentally. From this point of view the constancy of s with stress level is understandable for single fibres.

In his model for the kinetic failure of a Kevlar crystal as a result of molecular chain scission, Phoenix [3] assumed a bond energy of $3.35 \times 10^5 \, \text{J mol}^{-1}$ ($80 \, \text{kcal mol}^{-1}$) for the failure of C–N bonds and predicted $\varrho = 54$ at room temperature. While this value falls in the middle of the ϱ values in Fig. 6, one cannot conclude that chain scission is the dominant failure process. In any case it may be worthwhile modifying the model to include chain slippage as well as scission to see if decreasing values of ϱ with increased time scale can be predicted. Including other creep effects as described in Ericksen [10] may also be worthwhile.

Finally, the model in [3] does not predict massive chain scission in Kevlar filaments loaded to failure, and in fact predicts that less than one C–N bond in 10^{10} will be failed in regions away from the fracture surface. Thus the meagre evidence of chain scission in the study of Brown *et al.* [11] does not in our opinion rule out chain scission as the dominant molecular failure process in Kevlar.

Lifetime experiments at elevated temperatures are underway and will be reported on later.

5. Conclusions

We have conducted an experimental study on the creep-rupture of single Kevlar 49 filaments, and consider the major conclusions to be as follows:

1. The lifetimes of single Kevlar 49 filaments follow a two-parameter Weibull distribution with shape parameter near 0.2, as predicted theoretically.

2. At the same absolute stress level, filaments taken from two spools which earlier showed a 7% difference in median filament strength also showed a corresponding difference in median lifetime of about an order of magnitude.

3. At the same stress ratio (stress level divided by Weibull scale parameter for short-term strength) the Weibull lifetime distributions for filaments from the two spools differed insignificantly.

4. The dependence of lifetime on stress level was according to a power law within each of three distinct time domains with three different power-law exponents. The time domains and exponents were in excellent agreement with those observed by other workers for preproduction Kevlar 49/epoxy strands.

References

1. S. L. PHOENIX and E. M. WU, "Statistics for the Time-Dependent Failure of Kevlar 49/Epoxy Composites: Micromechanical Modeling and Data Interpretation", Report No. UCRL-53365, (Lawrence Livermore National Laboratory, Livermore, California, 1983).
2. S. L. PHOENIX, *Int. J. Fracture* **14** (1978) 327.
3. *Idem*, Statistical Modeling of the Time and Temperature Dependent Failure of Fibrous Composites, in Proceedings of the Ninth US National Congress of Applied Mechanics, Book no. H00228 (The American Society of Mechanical Engineers, New York, 1982) p. 219.
4. S. L. PHOENIX and L-J. TIERNEY, *Eng. Fract. Mech.* **18** (1983) 193.
5. S. L. PHOENIX and C. C. KUO, Recent Advances in Statistical and Micromechanical Modeling of the Time Dependent Failure of Fibrous Composites, in 1983 Advances in Aerospace Structures, Materials and Dynamics -AD-06,

Book no. H00272 (The American Society of Mechanical Engineers, New York, 1983) p. 169.
6. M. G. DOBB, D. J. JOHNSON and B. P. SAVILLE, *J. Polym. Sci. Polym. Phys. Ed.* **15** (1977) 2201.
7. M. G. DOBB, D. J. JOHNSON, A. MAJEED and B. P. SAVILLE, *Polymer* **20** (1980) 1284.
8. R. J. MORGAN, C. O. PRUNEDA and W. J. STEELE, *J. Polym. Sci Polym. Phys. Ed.* **21** (1983) 1757.
9. M. G. NORTHOLT, *Polymer* **21** (1980) 1199.
10. R. H. ERICKSEN, *ibid.* **26** (1985) 733.
11. I. M. BROWN, T. C. SANDRECZKI and R. J. MORGAN, *ibid.* **25** (1984) 759.
12. B. D. COLEMAN and A. G. KNOX, *Text. Res. J.* **27** (1957) 393.
13. B. D. COLEMAN, *J. Polym. Sci.* **20** (1956) 447.
14. R. E. WILFONG and J. ZIMMERMAN, *J. Appl. Polym. Sci. Appl. Polym. Symp.* **31** (1977) 1.
15. H. EYRING, *J. Chem. Phys.* **4** (1936) 283.
16. A. TOBOLSKY and H. EYRING, *ibid.* **11** (1943) 125.
17. B. D. COLEMAN, *J. Appl. Phys.* **27** (1956) 862.
18. S. N. ZHURKOV, *Int. J. Fract. Mech.* **1** (1965) 311.
19. S. N. ZHURKOV and V. E. KORSUKOV, *J. Polym. Sci. Polym. Phys. Ed.* **12** (1974) 385.
20. Y. Y. GOTLIB, A. V. DOBRODUMOV, A. M. EL'-YASHEVICH and Y. E. SVETLOV, *Sov. Phys. Solid State* **15** (1973) 555.
21. A. V. DOBRODUMOV and A. M. EL'YASHEVICH, *ibid.* **15** (1973) 1259.
22. C. B. HENDERSON, P. H. GRAHAM and C. N. ROBINSON, *Int. J. Fract. Mech.* **6** (1970) 33.
23. J. SMOOK, W. HAMERSMA and A. J. PENNINGS, *J. Mater. Sci.* **19** (1984) 1359.
24. W. A. STEPANOV and V. V. SHPEIZMAN, *Mater. Sci. Eng.* **49** (1981) 195.
25. D. C. PREVORSEK and W. J. LYONS, *J. Appl. Phys.* **35** (1964) 3152.
26. D. C. PREVORSEK, *J. Polym. Sci. Symp.* **32** (1971) 343.
27. R. M. CHRISTENSEN, *J. Rheol.* **25** (1981) 517.
28. R. M. CHRISTENSEN and R. E. GLASER, *J. Appl. Mech.* **52** (1985) 1.
29. R. E. GLASER, R. M. CHRISTENSEN and T. T. CHIAO, *Comp. Tech. Rev.* (1985) submitted.
30. R. M. CHRISTENSEN, *Int. J. Solids Struct.* **20** (1984) 791.
31. H. D. WAGNER, S. L. PHOENIX and P. SCHWARTZ, *J. Compos. Mat.* **18** (1984) 312.
32. F. P. GERSTLE and S. G. KUNZ, in "Prediction of Long-Term Failure in Kevlar 49 Composites, in Proceedings of ASTM Symposium on Long-Term Behavior of Composites", ASTM STP 813 (American Society for Testing and Materials, Philadelphia, Pennsylvania, 1983).
33. B. D. COLEMAN, *J. Appl. Phys.* **29** (1958) 968.
34. *Idem, Trans. Soc. Rheol.* **1** (1957) 153.
35. *Idem, ibid.* **2** (1958) 195.
36. W. NELSON, "Applied Life Data Analysis" (Wiley, New York, 1982).
37. W. Q. MEEKER and W. NELSON, *Technometrics* **19** (1977) 473.
38. D. R. THOMAN and L. J. BAIN, *ibid.* **11** (1969) 805.